European Journal of Microbiology and Immunology 3 (2013) 3, pp. 198–203
DOI: 10.1556/EuJMI.3.2013.3.8

ACTIN ASSESSMENT IN ADDITION TO SPECIFIC IMMUNO-FLUORESCENCE STAINING TO DEMONSTRATE RICKETTSIAL GROWTH IN CELL CULTURE

Hagen Frickmann[1,2,*,&], Elmar Schröpfer[3,&,#] and Gerhard Dobler[3]

[1]Department of Tropical Medicine at the Bernhard Nocht Institute, German Armed Forces Hospital of Hamburg, Germany
[2]Institute for Microbiology, Virology and Hygiene, University Hospital Rostock, Germany
[3]Institute for Microbiology of the German Armed Forces, Munich, Germany

Received: May 24, 2013; Accepted: June 8, 2013

Rickettsiae are able to spread within infected cell mono-layers by modifying intra-cellular actin formations. The study analyzes whether a visualization of actin modifications in addition to specific immuno-fluorescence staining of rickettsiae might facilitate the proof of rickettsial growth in cell culture.

Cell mono-layers of Vero E6 und BGM cells were infected with *Rickettsia honei*. Intra-cellular actin was fluorescence stained with TRITC-(tetra-methyl-5,6-isothiocyanate)-labeled phalloidin in addition to specific immuno-fluorescence staining of rickettsiae with FITC-(fluorescein-isothiocyanate)-labeled antibodies. DNA of bacteria and cells was counter-stained with DAPI (4′,6-diamino-2-phenyl-indole). Cell cultures infected with Vaccinia virus were used as positive controls, cell cultures infected with *Coxiella burnetii* as negative controls.

High concentrations of *R. honei* are necessary to demonstrate characteristic modifications of the intra-cellular actin. This effect is more pronounced in Vero E6 cells than in BGM cells.

Actin staining with phalloidin is not suited for an early proof of rickettsial growth in cell culture but may confirm unclear findings in specific immuno-fluorescence staining in case of sufficient bacterial density.

Keywords: rickettsiae, actin, phalloidin, cell culture, diagnostics

Introduction

Rickettsiae are bacterial pathogens showing obligatorily intra-cellular growth. Cell culture protocols for culture-based diagnosis of rickettsial infections are available in specialized laboratories only. Laborious and time-consuming quantitative nucleic acid amplification (NAT)-based procedures from the cell culture broth or microscopic detection of rickettsiae by Giemenez or immuno-fluorescence staining in the cell mono-layer allow for the proof of rickettsial growth in culture. However, microscopic identification of the very small microorganisms and discrimination from artefacts requires a high degree of expertise. Therefore, confirmatory counter-staining by using alternative fluorescence channels is desirable to reduce false-positive results. One option is the demonstration of bacterial DNA at the sites of immuno-fluorescence using the non-intercalating DNA stain 4′,6-Diamino-2-phenylindole (DAPI). Another one is the analysis of infection-induced effects on the actin structure of infected cells.

Rickettsiae of the spotted fever group as well as *Rickettsia typhi,* a species of the typhus group, spread from cell to cell by so-called actin-based mobility (ABM), i.e., an induced restructuring of intra-cellular actin. Actin tails, i.e., filamentous F-actin polymers, are developed during this mode of spreading [1, 2] *(Fig. 1)*. The helical coiling of the individual actin bundles around each other causes a forward movement of the rickettsiae by rotation [1]. This actin polymerization-driven locomotion moves the rickettsiae through the cytosol of their host cells into protrusions of the cellular membranes, thus allowing for incorporation into neighboring cells or discharge into the culture medium [3, 4]. The temporal dynamics of actin tail formation are species-specific [1, 3, 5]. The half life of actin tails is not longer than a few minutes [6], marking their detection as a stochastical phenomenon.

*Corresponding author: Hagen Frickmann; Department of Tropical Medicine at the Bernhard Nocht Institute, German Armed Forces Hospital of Hamburg, Bernhard Nocht street 74, D-20359 Germany; Phone: 0049-40-6947-28743; Fax: 0049-40-6947-28709; E-mail: Frickmann@bni-hamburg.de

[&] Hagen Frickmann and Elmar Schröpfer contributed equally to this work.

[#] Retired.

ISSN 2062-509X / $ 20.00 © 2013 Akadémiai Kiadó, Budapest

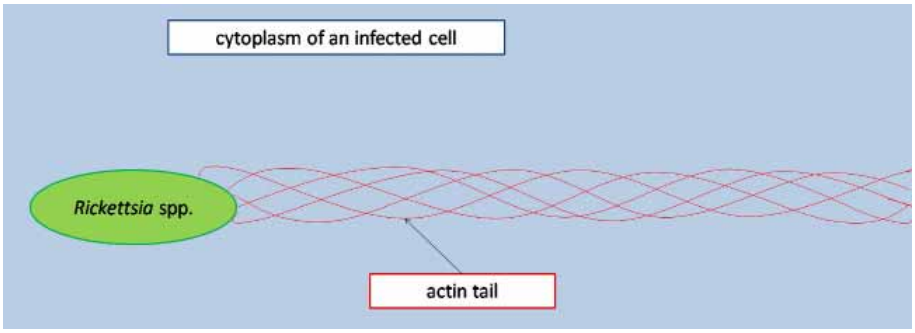

Fig. 1. Scheme of a rickettsial cell with actin tail in an infected host cell

Next to rickettsiae, also Vaccinia virus and facultative intra-cellular bacteria like *Listeria* spp. and *Shigella* spp. are able to induce actin tails [5], while closely related *Coxiella burnetii* do not induce actin tails in spite of transient affections of the cytoskeleton of their target cells after internalization [1, 7].

Irrespective of pathogen-induced changes of the cytoskeleton, many cells are able to form so-called stress fibers in cell culture, contractile elements, which are mainly basally located, consist of aligned micro-filament bundles and make the assessment of cytoskeleton affections more challenging [8].

This study deals with the question, whether and in how far screenings for pathogen-induced affections of the cytoskeleton are useful and easy-to-perform additions to immuno-fluorescence for the proof of rickettsial growth in cell culture, irrespective of their poor specificity [1, 5].

Materials and methods

Model organism was the bio-safety level (BSL) 2 strain *Rickettsia honei* (ATCC VR-1472). It was grown on confluent mono-layers of kidney parenchyma cells of green monkeys (cell lines BGM and Vero E6). Both Vero E6 cells and BGM cells are prone to expressing stress fibers under culture conditions.

R. honei was inoculated in concentrations of 10^2 to 10^6 tissue culture infecting doses (TCID). Growth was performed in so-called slide flasks, i.e., cell culture bottles with a slide at the bottom. Culture medium was minimal essential medium (MEM) by Gibco (Invitrogen Ltd., Karlsruhe, Germany) enriched with 5% inactivated foetal calf serum (FCS) and 1% non-essential amino acids (NEA). Non-infected slide flasks were used as negative controls for each experiment. Rickettsial growth in the infected cell lines was morphologically confirmed by complete cytopathic effects next to molecular confirmation by NAT targeting the *gltA* gene as described [9] for each experimental setting. Inactivation of rickettsiae with 10% formalin with which all slide flasks were filled after removal of the culture medium was performed 24 h and 48 h after infection.

After the inactivation procedure, all samples were washed three times for 2 min with PBS (phosphate-buffered saline) and permeabilized for 10 min with 0.1% Triton X-100 (Sigma Aldrich, Steinheim, Germany). An additional washing with PBS three times for 2 min followed to remove remaining Triton X-100 from the flasks prior to the staining procedure. No blocking solution, e.g., 3% milk powder in PBS, was used to avoid streaking. The slides were cut in half prior to all staining procedures to preserve reserve samples for the case of failed staining. If immediate staining after inactivation and permeabilization was not possible for organizational reasons, the slide flasks were filled with PBS and stored at 4 °C.

The staining procedure included a triple-fluorescence staining of the slides. At first, the slides were incubated with human IgG antibodies (Fuller, Fullerton, CA) against *Rickettsia conorii*, a species of spotted-fever group same as *R. honei*. Serological cross-reaction can be expected within the spotted-fever group. In detail, the anti-rickettsiae antibody was diluted 2 : 3 in PBS. Afterwards, a 30 µl volume was applied to each half slide and covered by a cover slide. Incubation was performed in a moist chamber at 37 °C for 1 h in the dark. Then, the slides were washed with little distilled water.

Then the rickettsiae were visualized by immuno-fluorescence with FITC-(fluorescein-isothiocyanate)-labeled (absorption maximum: 492 nm, emission maximum: 520–530 nm, green fluorescence) rabbit anti-human IgG Fab2 antibodies (DakoCytomation, Glostrup, Denmark) in a dilution of 1 : 20 in PBS. Again, a 30 µl volume was applied to each half slide and covered by a cover slide, followed by incubation at 37 °C in the moist chamber for 1 h in the dark and consecutive washing with distilled water.

TRITC-(tetramethylrhodamine-5,6-isothiocyanate)-labelled (absorption maximum: 537 nm, emission maximum: 566 nm, orange fluorescence) phalloidin (Sigma Aldrich, Steinheim, Germany) was used to stain the actin cytoskeleton of the cells. TRITC-phalloidin was diluted 1 : 10 in PBS, a 30 µl volume was applied to each half slide and covered by a cover slide, followed by storage in the moist chamber for 1 h at room temperature in the dark and consecutive washing with little distilled water.

Afterwards, the mounting medium "Vectashield with DAPI" (4´,6-Diamino-2-phenylindole, Vector Laboratories, Burlingame, CA, absorption maximum: 358 nm, emission maximum: 461 nm, blue fluorescence) was used to cover the slides, thus visualizing DNA of cells and bacteria by the non-intercalating DNA-stain DAPI.

For some samples, immuno-fluorescence was not performed and instead the actin cytoskeleton was stained with FITC-labeled phalloidin (Sigma Aldrich, Steinheim, Germany). In these instances, presence and position of rickettsiae were demonstrated by visualizing their DNA with DAPI. The order of immuno-fluorescence staining and

actin staining did not affect the quality of the staining as shown in prior experiments (data not shown).

The efficiency of the staining method for the demonstration of pathogen-induced actin tails was confirmed using the Vaccinia virus strain ELSTREE on MA-104 cells as a positive control [5]. The *Coxiella burnetii* strain NineMile was grown under BSL-3 conditions on BGM cells as negative control. Positive and negative controls were inactivated and stained after intra-cellular growth for 48 h as described for the rickettsiae. Different from the protocol for the rickettsiae, immuno-fluorescence staining of *C. burnetii* and fluorescence staining of the cytoskeleton of the BGM cells were performed simultaneously. To do so, 0.8 µl of the directly conjugated monoclonal antibody MAB 3.13 (co-operation with Squarix, Marl, Germany, conjugated with green-fluorescing Oregon green by Invitrogen Ltd., Karlsruhe, Germany) and 3 µl TRITC-phalloidin were mixed with 30 µl PBS and applied to each half slide. Afterwards, the slide was covered by a cover slide and incubated in a moist chamber for 1 h at room temperature.

The stained samples were assessed with a fluorescence microscope (Zeiss, Jena, Germany). Morphological changes of the cytoskeleton of infected cell cultures were compared with non-infected negative control cell mono-layers which were exposed to the same inactivation, permeabilization and staining procedures as the infected samples. Visually detectable changes of phalloidin-stained intracellular actin formations were assessed in comparison with these negative controls.

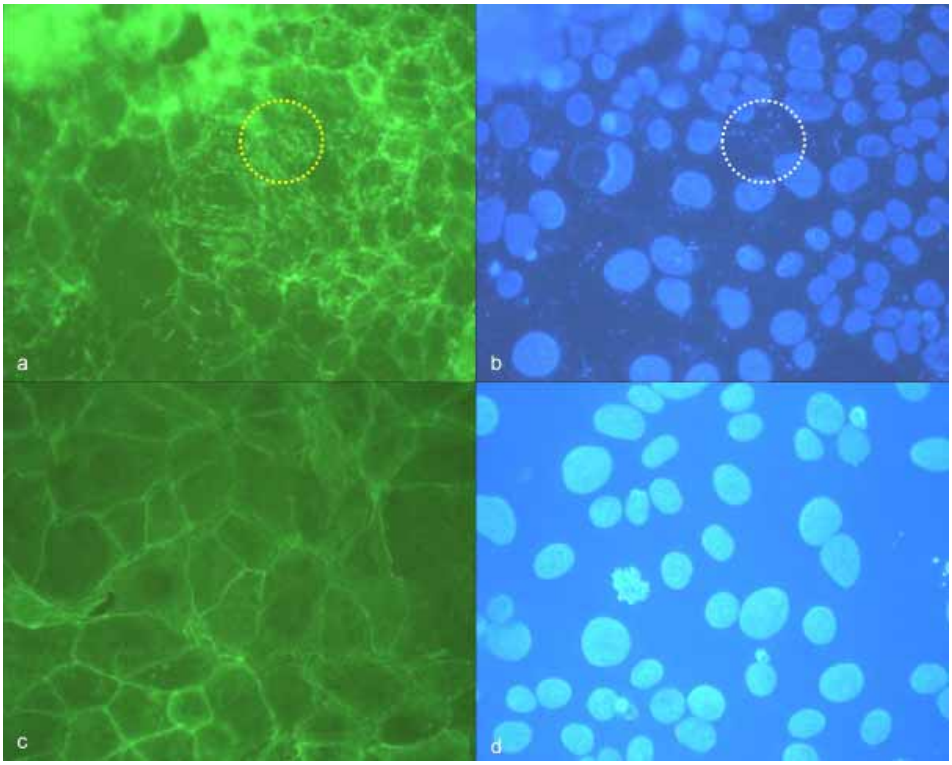

Fig. 2. (a) High density of *R. honei* in Vero E6 cells, 48 h after infection, phalloidin-FITC staining of actin, yellow circle: stained actin polymerization (green); (b) corresponding position to (a), DAPI staining of DNA, white circle: punctiform nucleic acids of rickettsiae; (c) negative control Vero E6 cells, phalloidin-FITC staining of actin, (d) corresponding position to (c), DAPI staining of nucleic acids

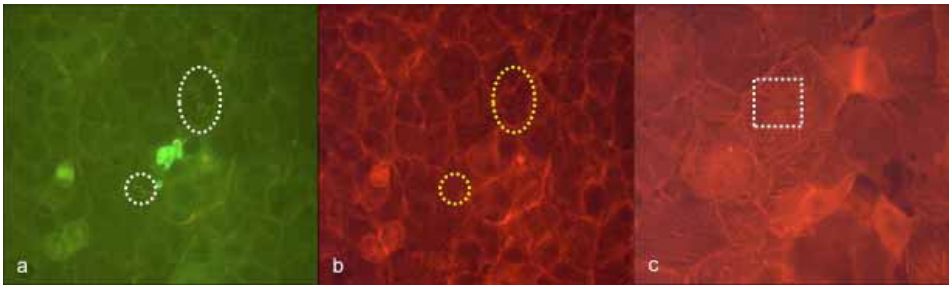

Fig. 3. (a) Low density of *R. honei* in Vero E6 cells, 24 h after infection, immuno-fluorescence staining, white circle and white oval: stained rickettsiae (green); (b) corresponding position to (a), phalloidin-TRITC staining of actin, yellow circle and yellow oval: only weak staining (orange) indicating diffuse actin polymerization; (c) negative control Vero E6 cells, phalloidin-TRITC staining of actin, white rectangle: stress fibers in non-infected Vero E6 cells

The presented figures were partly merged from single shots of the fluorescence channels for DAPI (band pass filter (BP): 365/12 nm, long pass filter (LP): 397 nm, fluorescence threshold (FT): 395 nm), FITC (band pass filter (BP): 450-490 nm, long pass filter (LP): 519 nm, fluorescence threshold (FT): 510 nm) and rhodamine (band pass filter (BP): 546/12 nm, long pass filter (LP): 590 nm, fluorescence threshold (FT): 580 nm) to reduce the number of figures and for the sake of better representability. The merging was performed using the software EclipseNet Laboratory Imaging V. 1.20.

Results

Morphological changes of cytoskeleton architecture depended on the infectious dose. *R. honei*-induced changes of the cytoskeleton of Vero E6 cells were clearly visible 24 and 48 h after infection if 10^5 to 10^6 TCID were used. Massive filiform actin polymerization corresponded with diffusely disseminated intracellular nuclei of rickettsiae in DAPI stain *(Fig. 2a,b)*. Respective changes were not detectable on negative control slides *(Fig. 2c,d)*. Accordingly, the tail-like actin polymerization was likely to be caused by rickettsial spreading.

In contrast, filiform restructuring of the cytoskeleton corresponding to rickettsial antigens in immuno-fluorescence was hardly detectable 24 h after rickettsial infections with no more than 10^2 to 10^3 TCID in Vero E6 cells. Only weakly visible actin polymerization was observed at positions corresponding to intra-cellular rickettsiae. However, a reliable discrimination from artefacts was not possible in these instances *(Fig. 3a,b)*.

Interestingly, infection with *R. honei* led to a nearly total vanishing of stress fibers in Vero E6 cell culture 24 h after infection in comparison with negative control slides. In non-infected Vero E6 cell mono-layers, stress fibers are basally arranged. Not only densely infected cells showed the phenomenon of the vanished stress fibers. It was nearly ubiquitously detectable in the infected Vero E6 cell mono-layer *(Fig. 3b,c)*.

BGM cells, however, were less suitable for the demonstration of *R. honei*-induced changes of the cytoskeleton. In BGM cells, stress fibers persisted 24 h after infection with *R. honei* and there was no difference compared with negative control slides *(Fig. 4a–f)*. Only decent punctiform to diffuse actin polymerization in association with rickettsial antigens was visible in BGM cell mono-layers 24 h after *R. honei* infections even with high infectious doses of 10^5 to 10^6 TCID *(Fig. 4a,b,d,e)*. A reliable discrimination from artefacts was not possible.

The positive control slides carrying MA-104 cells infected with Vaccinia virus showed extensive modifications of the cytoskeleton, including actin tail formation as expected *(Fig. 5)*. The negative control slides carrying BGM cells infected with *C. burnetii* showed nearly no changes of the cytoskeleton 48 h up to 2 weeks after infection. Stress fibers that are typical for BGM cells in cell culture were visible without any association to the intra-cellular bacteria *(Fig. 6a)*. However, clearings of the fiber network were detectable around vacuoles filled with *C. burnetii (Fig. 6b,c)*. Vero E6 cells infected with *C. burnetii* tended to detach-

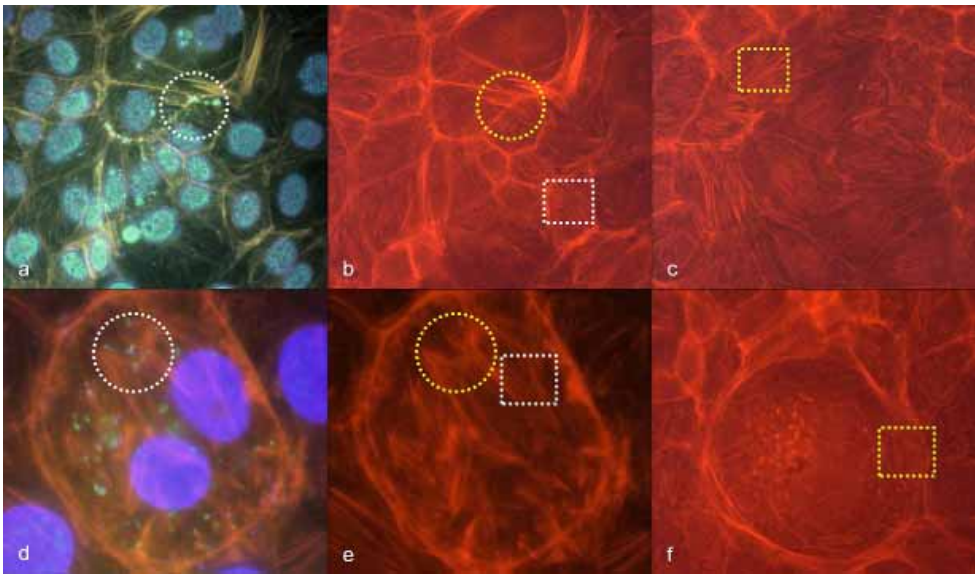

Fig. 4. (a) High density of *R. honei* in BGM cells, 24 h after infection, immuno-fluorescence staining (green to turquoise), phalloidin-TRITC staining of actin (orange), DAPI staining of DNA (blue), white circle: stained rickettsiae (green) with polymerized actin (orange); (b) corresponding position to (a), phalloidin-TRITC staining of actin, yellow circle: polymerized actin (orange), white rectangle: stress fibers (orange); (c) negative control BGM cells, phalloidin-TRITC staining of actin, yellow rectangle: stress fibers (orange); (d) high density of *R. honei* in BGM cells, 24 h after infection, immuno-fluorescence staining (green to turquois), phalloidin-TRITC staining of actin (orange), DAPI staining of DNA (blue), white circle: stained rickettsiae (green) with polymerized actin (orange); (e) corresponding position to (d), phalloidin-TRITC staining of actin, yellow circle: polymerized actin (orange), white rectangle: stress fibers (orange); (f) BGM cell without *R. honei* infection, yellow rectangle: stress fibers (orange)

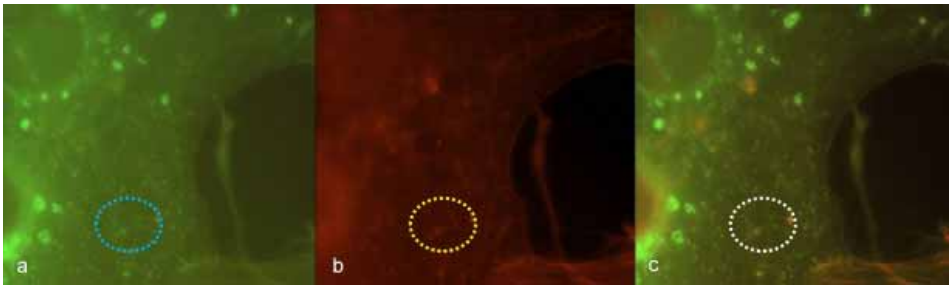

Fig. 5. (a) Vaccinia virus (strain *ELSTREE*) in MA-104 cells, 48 h after infection, immuno-fluorescence staining, blue oval: immuno-stained Vaccinia virus (green); (b) corresponding position to (a), phalloidin-TRITC staining of actin, yellow oval: actin tails (orange); (c) corresponding position to (a) and (b), merged picture, immuno-fluorescence (green to turquoise), phalloidin-TRITC staining of actin (orange), white oval: actin tails (orange) and Vaccinia virus (green) at corresponding positions

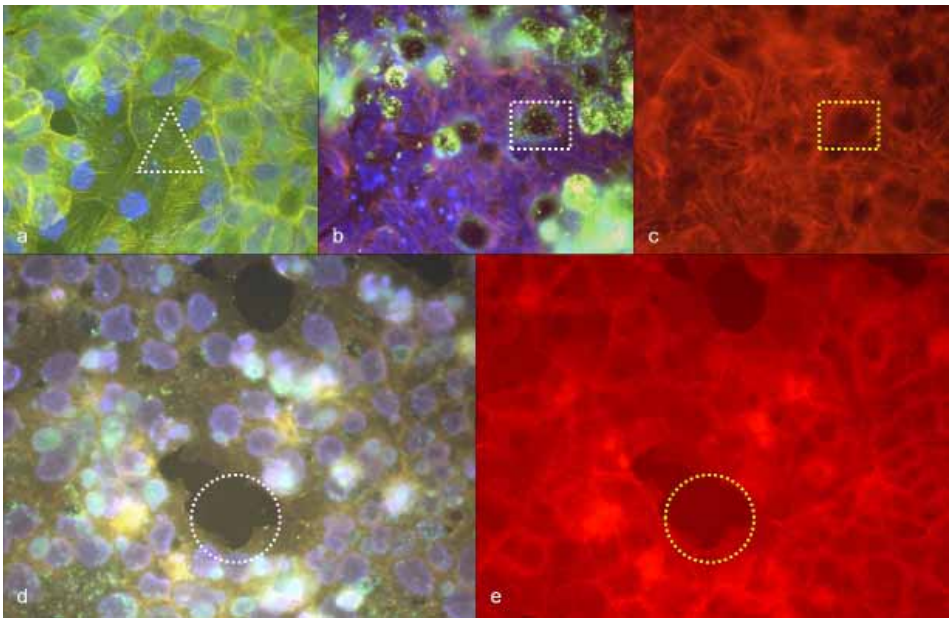

Fig. 6. (a) *C. burnetii* in BGM cells, 48 h after infection, immuno-fluorescence staining (green), phalloidin-TRITC staining of actin (yellow), DAPI staining of DNA (blue), white triangle: stress fibers (yellow) without detectable association to immuno-stained *C. burnetii* (green); (b) *C. burnetii* in BGM cells, 48 h after infection, immuno-fluorescence staining (green), phalloidin-TRITC staining of actin (orange), DAPI staining of DNA (blue), white rectangle: immuno-stained *C. burnetii* (green) in a vacuole; (c) corresponding position to (b), phalloidin-TRITC staining of actin, yellow rectangle: absence of stress fibers around the vacuole; (d) *C. burnetii* in Vero E6 cells, 48 h after infection, immuno-fluorescence staining (green to turquoise in vacuoles), phalloidin-TRITC staining of actin (orange), DAPI staining of DNA (violet), white circle: detachment of infected cells; (e) corresponding position to (d), phalloidin-TRITC staining of actin, yellow circle: detachment of infected cells

ment from the cell mono-layer *(Fig. 6d,e)*. Apart from this, infection with *C. burnetii* did not lead to reliably detectable changes of the cytoskeleton of Vero E6 cells *(Fig. 6d,e)*.

Discussion

Extensive filiform restructuring of the cytoskeleton could only be achieved with high infectious doses of *R. honei* in cell culture, predominantly affecting intra-cellular actin formations in Vero E6 cells. Infections with low TCID, in contrast, did not lead to detectable effects even 24 h after infection.

However, even in heavily infected cell mono-layers, characteristic actin tails were not identified in cells infected by *R. honei*. Accordingly, a screening for actin tails to confirm the growth of rickettsiae of the spotted fever group in cell cultures is not promising as a rapid diagnostic procedure. It remains unclear whether this is due to the short half life of the actin tails [6] or whether *R. honei* do not induce actin tails in contrast to other rickettsiae of the spotted fever group like, e.g., *R. conorii*. The vanishing of stress fibers in Vero E6 cells infected with *R. honei* indicates extensive restructuring of intracellular actin. However, the expression of stress fibers varies in non-infected Vero E6 cells as well, making this phenomenon unsuitable for the proof of rickettsial growth in culture. In BGM cells, it was not even detectable.

In summary, extensive restructuring of the cytoskeleton of Vero E6 cells provided additional hints for rickettsial growth in cell culture, but only in case of high bacterial density. Early stages of actin polymerization,

which can be punctiform or diffuse [1, 3], are difficult to discriminate from artefacts and therefore not useful for diagnostic purposes. The specificity of actin staining is low, because other pathogens like *Shigella* spp., *Listeria* spp., and Vaccinia virus can lead to comparable changes of actin formations [5]. However, phalloidin staining is rapid and easy-to-perform, allowing for a combination with specific immuno-fluorescence to confirm equivocal immuno-fluorescence results in cell culture by the demonstration of changed actin formations in comparison with non-infected negative control slides.

Acknowledgements

The authors are grateful to D. Frangoulidis and H. Meyer for providing the Vaccinia virus and *C. burnetii* strains which were used as positive and negative controls. Mrs. Kahlhofer, Mr. Lodri, and Mrs. Terzioglu are gratefully acknowledged for excellent technical assistance by performing the staining and the NAT analyses.

References

1. Goldberg MB: Actin-based motility of intracellular microbial pathogens. Microbiol Mol Biol Rev 65, 595–626 (2001)
2. Heinzen RA: Rickettsial actin-based motility: behavior and involvement of cytoskeletal regulators. Ann N Y Acad Sci 990, 535–547 (2003)
3. Heinzen RA, Hayes SF, Peacock MG, Hackstadt T: Directional actin polymerization associated with spotted fever group rickettsia infection of vero cells. Infect Immun 61, 1926–1935 (1993)
4. van Kirk LS, Hayes SF, Heinzen RA: Ultrastructure of *Rickettsia rickettsii* actin tails and localization of cytoskeletal proteins. Infect Immun 68, 4706–4713 (2000)
5. Gouin E, Gantelet H, Egile C, Lasa I, Ohayon H, Villiers V, Gounon P, Sansonetti PJ, Cossart P: A comparative study of the actin-based motilities of the pathogenic bacteria *Listeria monocytogenes*, *Shigella flexneri* and *Rickettsia conorii*. J Cell Sci 112 (Pt 11), 1697–1708 (1999)
6. Heinzen RA, Grieshaber SS, van Kirk LS, Devin CJ: Dynamics of actin-based movement by *Rickettsia rickettsii* in vero cells. Infect Immun 67, 4201–4207 (1999)
7. Meconi S, Jacomo V, Boquet P, Raoult D, Mege JL, Capo C: *Coxiella burnetii* induces reorganization of the actin cytoskeleton in human monocytes. Infect Immun 66, 5527–5533 (1998)
8. Sanger JW, Sanger JM, Jockusch BM: Differences in the stress fibers between fibroblasts and epithelial cells. J Cell Biol 96, 961–969 (1983)
9. Wölfel R, Terzioglu R, Kiessling J, Wilhelm S, Essbauer S, Pfeffer M, Dobler G: Rickettsia spp. in Ixodes ricinus ticks in Bavaria, Germany. Ann N Y Acad Sci 1078, 509–511 (2006)